

Edge morphology effect on field emission properties of graphene thin films

Yanlin Gao*, Susumu Okada

*Graduate School of Pure and Applied Sciences, University of Tsukuba, 1-1-1 Tennodai,
Tsukuba 305-8571, Japan*

Abstract

Field emission current density from the edge of graphene thin films are calculated in terms of their edge morphology, using the density functional theory combined with the effective screening medium method and the Fowler-Nordheim theory. The field emission current from the bilayer graphene edges is higher than that from the monolayer graphene edges. Edge displacement of the bilayer graphene causes the higher emission current than the aligned edges for both zigzag and armchair edges. Bilayer graphene with closed edges further enhances the emission current compared with those with open clean edges, owing to the decrease of their work function and the potential outside them.

Keywords: Field emission current, Bilayer graphene with edge displacement, Folded graphene, DFT

2010 MSC: 00-01, 99-00

1. Introduction

Nanocarbon materials, such as carbon nanotubes and graphene, are known to possess unusual electronic and mechanical properties arising from their dimensionality, size, and morphology. Two-dimensional honeycomb network of carbon atoms endows graphene with remarkable carrier mobility arising from pairs of linear dispersion bands at the Fermi level. By imposing the open boundary condition on graphene, resultant strips of graphene are either metals or semiconductors, depending on the edge atomic arrangement and the width, some of which show carrier concentration near the edge atomic sites caused by the peculiar edge-localized states. Curvature and topological defects also cause further variation in the electronic properties of the resultant graphene derivatives. Besides the electronic structures, the covalent network of sp^2 C atoms causes remarkable mechanical strength and high chemical stability of graphene and its derivatives. According to their physical and chemical properties arising from

*Corresponding author

Email address: ylgao@comas.frsc.tsukuba.ac.jp (Yanlin Gao)

15 the characteristic geometry, graphene and its derivatives, carbon nanotubes and graphene nanoflakes, are regarded as emerging materials for functional devices in the future technologies.

Among such applications, graphene and carbon nanotubes are considered to be suitable materials for emitting electrons, because of their high structural
20 aspect ratio, remarkable chemical stability, high mechanical stiffness, and excellent carrier conductivity. Indeed, graphene works as the electron emitting source with the high and stable current density under the low turn-on electric field [1, 2, 3, 4, 5, 6]. It has been experimentally reported that electrons are primarily emitted around atomic sites of graphene edge where electric field
25 concentration occurs. For the field emission from graphene edges, experimental and theoretical works have clarified that the emission current strongly depend on the edge morphologies and terminations [3, 4, 7, 8, 9, 10, 11, 12, 13]. Besides the monolayer graphene, graphene thin films are also plausible materials that provide high emission current from their edges under the electric field, owing
30 to their multiple structures. For example, few-layer graphene is found to be a good field emitter, with a turn-on fields as low as $1 \text{ V}/\mu\text{m}$ [6]. In the case of graphene thin film, there are additional edge morphology, such as edge dislodgement [14, 15, 16, 17, 18] and open/closed edges [19, 18, 20], which certainly affects the emission properties in addition to the edge atomic arrangements and
35 terminations. Although several experiments provide fragmentary knowledge of those problems, comprehensive theoretical studies on the emission current from graphene thin films in terms of their edge morphology are still absent to date.

Based on the above background, in this paper, we aim to provide the theoretical insight into the field emission properties of graphene thin films under
40 an external electric field in terms of their the edge morphology arising from their multilayered structures, based on the density functional theory (DFT) combined with the Fowler-Nordheim theory and the effective screening medium (ESM) method on bilayer graphene with various edge morphologies. Our DFT calculations showed that the emission current from bilayer graphene are sensitive
45 to the edge morphologies: bilayer graphene with armchair edges provides higher emission current than those with zigzag edges, owing to the lower potential barriers outside the edges. For both kinds of edges, the emission current monotonically increases with increasing the amount of edge dislodgements. Furthermore, the edge closing of the bilayer graphene causes further increase in the
50 emission current. This manuscript is organized as following. In section 2, theoretical methods used in this work are expressed. The detail of structural models studied in this work is explained in section 3. Results and discussion are given in section 4. The manuscript is summarized in section 5.

2. Calculation methods

55 All calculations in this study were based on the DFT [21, 22] implemented in the Simulation Tool for Atom TEchnology (STATE) package [23]. The exchange-correlation potential among interacting electrons was treated using

the generalized gradient approximation with the Perdew-Burke-Ernzerhof functional [24]. The interaction between electrons and ions was described by ultrasoft pseudopotentials generated by the Vanderbilt scheme [25]. The valence wave function and deficit charge densities were expanded in terms of plane-wave basis sets with cut-off energies of 25 and 225 Ry, respectively. All atomic structures were optimized until the force on each atom was below 5 mRy/Å under the zero-electric-field condition except the cases of bilayer graphene with closed edges. For the bilayer graphene with closed edges, two atomic lines at the open edge side are fixed to retain their folded structure at the other side. Integration over the Brillouin zone was carried out using a sampling with 4- k points along the edge direction, which enabled sufficient convergence in the total energy and electronic structures of graphene [26]. All atomic structures were fixed as those under zero-electric field during the calculations of electronic properties under an external electric field.

The ESM method was used to investigate the electrostatic potential properties of bilayer graphene under the lateral electric field. Figs 1(a) and 1(b) show the calculation models of bilayer graphene with the open and closed edges, respectively, under the external lateral electric field, where electrons are injected into the bilayer graphene by the planar counter metal electrodes described by an infinite relative permittivity using the ESM method, and the edges of the bilayer graphene facing the electrode are separated by a 5 Å vacuum spacing from the electrode. In contrast, an open boundary condition is imposed at the opposite cell boundary described by a relative permittivity of 1 with the vacuum spacing of 5 Å from the other edges, where C atoms are terminated by the H atoms to simulate the bilayer graphene with the infinite width.

3. Structural models

For the bilayer graphene with the open edges, we considered bilayer armchair and zigzag graphene nanoribbons (AGNRs and ZGNRs) with the width of 15.76 and 15.47 Å, respectively, and interlayer spacing of 3.4 Å in the AB stacking arrangement. To investigate the edge dislodgment effects, the one of two edges is protruded by t_X , where $X = A$ for the armchair edge and $X = Z$ for the zigzag edge. We consider the bilayer AGNRs with $t_A=0, 1.23, \text{ and } 2.46$ Å and bilayer ZGNRs with $t_Z=0.72, 1.44, \text{ and } 2.87$ Å. As for the bilayer graphene with closed edges, we considered the folded GNRs with armchair and zigzag edges which are terminated by H atoms. Fig. 3 shows the optimized geometries of folded GNRs with armchair or zigzag edges, whose curvature radius of the folded moiety is r_X , where $X = A$ for the folded AGNR and $X = Z$ for the folded ZGNR. The r_A of the optimized folded AGNRs is 1.98, 3.17, and 3.64 Å, respectively, and r_Z of folded ZGNRs 2.89, 2.93, and 3.37 Å respectively.

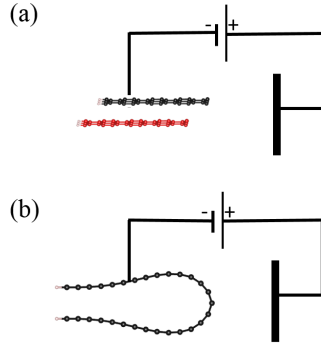


Figure 1: The calculation models of (a) bilayer GNRs and (b) folded GNRs under a lateral external electric field.

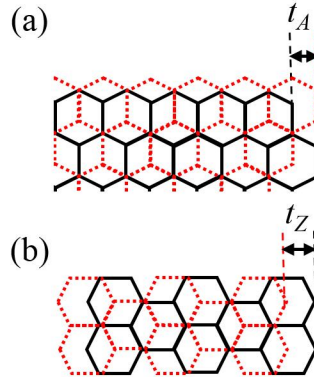


Figure 2: The geometric structures of bilayer (a) AGNRs and (b) ZGNRs with a lateral displacement of t_A and t_Z , respectively.

4. Results and discussion

4.1. Bilayer graphene with closed edges

Table 1 shows the work functions of bilayer graphene with armchair and zigzag edges whose edges possess dislodgements. The work functions of armchair edges of bilayer graphene with the dislodgment of 0, 1.23, and 2.46 Å are 5.20, 5.25, and 5.15 eV, respectively, which are smaller than 5.38 eV of armchair edge of monolayer graphene. For the zigzag edges, the work functions are 5.93, 5.90, and 5.83 eV for the edge dislodgements of 0.72, 1.44, and 2.87 Å, respectively, which are also smaller than 6.34 eV of the monolayer graphene. The work function of bilayer graphene depends on the edge shape and the lateral displacement t_X . The zigzag edges have higher work function than armchair edges, consistent with the case of monolayer graphene. For both kinds of edges, the work function monotonically decreases with increasing the edge displacement t_X . These results imply that edges of bilayer graphene cause higher emission current than those of monolayer graphene. In order to confirm the field emission

Table 1: Work function of AGNRs and ZGNRs with clean and functionalized edges.

	$X = A$			$X = Z$		
Dislgment t_X (Å)	0	1.23	2.46	0.72	1.44	2.89
Φ (eV)	5.20	5.25	5.15	5.93	5.90	5.83

property of bilayer graphene with the open edges, we calculated the potential barriers outside the edges for the electron emission and the emission current density under the external electric field. The current density I was evaluated based on the Fowler-Nordheim theory by using the relation

$$I = \lambda\nu \exp\left[\frac{-4\pi}{h} \int \sqrt{2m(V(z) - E_F)} dz\right], \quad (1)$$

where λ is the electron density accumulated near the edge by the external electric field, ν is the collision frequency of electrons estimated by $\nu = E_k/h$ with the electron kinetic energy E_k , and $V(z)$ is the plane-averaged electrostatic potential across the bilayer graphene. Figs. 4(a) and 4(b) are the potential barrier and field emission current of bilayer graphene with open edges, respectively, as a function of the external electric field. The potential barrier and emission current depend on the intensity of the electric field, edge shape, and edge displacement. The potential barrier for all bilayer graphene decreases with increasing the electric field. As for the edge morphology, the potential barrier for the armchair edges is lower than that for the zigzag edges, in accordance with the work function difference. For both kinds of edges, the potential barrier decreases with the increase in the edge displacement t_X . In addition, bilayer graphene has lower potential barrier than monolayer graphene. Accordingly, the field emission current also depends on the edge shape, edge displacement, and electric field: the current monotonically increases with increasing the electric field, the armchair edges result in higher current than the zigzag edges, and the edge dislodgement slightly enhances the current. Furthermore, the bilayer graphene causes substantially higher emission current than the monolayer graphene.

Field emission properties of materials are affected by the electrostatic potential and electric field around the emitting sites. Therefore, we depict the contour plot of the electrostatic potential and the vector plot of the field of bilayer graphene with the open edge and various edge displacement t_X (Fig. 4). The electrostatic potential outside the bilayer graphene monotonically decreases with approaching to the electrode. Note that the electrostatic potential is depicted by taking the difference between the potential under the critical electric field at which the electrostatic potential on the electrode crosses the Fermi level with excess electron of 0.1 electrons and that without the electron to exclude the deep potential arising from ions. The electric field mainly concentrated around the edges sites facing to the electrode. The distributions of the electrostatic potential and electric field are sensitive to the edge dislodgement. The electric field is highly concentrated at the protruded edges, so that the field concentration monotonically enhances with the increase in the edge displacement t_X .

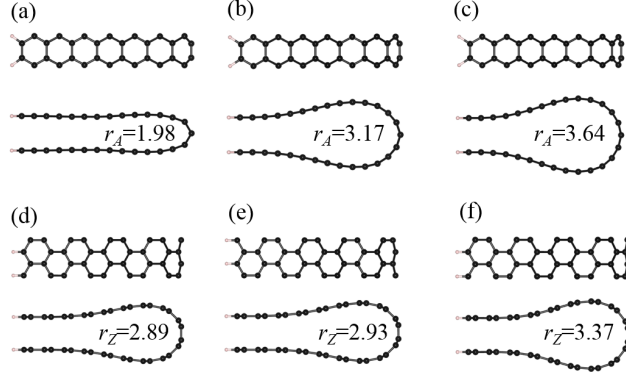


Figure 3: Optimized geometries of folded GNRs with different curvatures

The field concentration near the protruded edges is the physical origin why the field emission current enhances upon the increases of the edge dislodgement t_X .

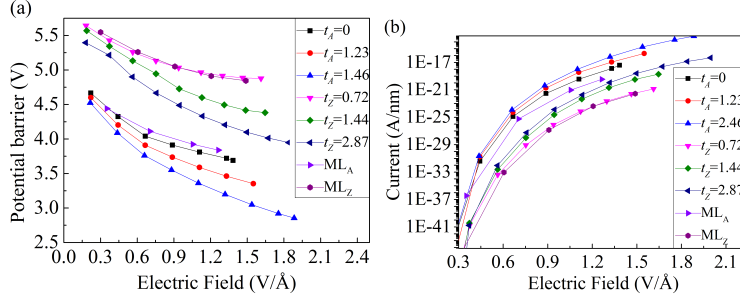


Figure 4: Electric-field dependence of (a) the potential barrier and (b) field emission current for the field emission of bilayer and monolayer GNRs with clean edges.

The electron density around the emission sites is another important parameter for determining the emission current, in addition to the work function and local electric field. Fig. 6 shows the distributions of accumulated electrons across the bilayer graphene with the open zigzag and armchair edges under the external electric field injecting 0.1 electrons into the graphene. We found that the injected electrons are primarily distributed around the edge atomic sites of which distribution depends on the edge shapes and dislodgement t_X . For the armchair edges, carriers are not only accumulated near the edge atomic sites but also slightly penetrated inside graphene, while, for the zigzag edges, the carrier concentrations occur near the edge atomic sites, suggesting that these atoms contribute to the field emission. By integrating the accumulated carrier around the edge atomic sites, carrier density of the bilayer graphene is about 0.09 electrons irrespective of the edge displacement, so that the enhancement of the emission current is mainly ascribed to the field concentration around the protruded edges.

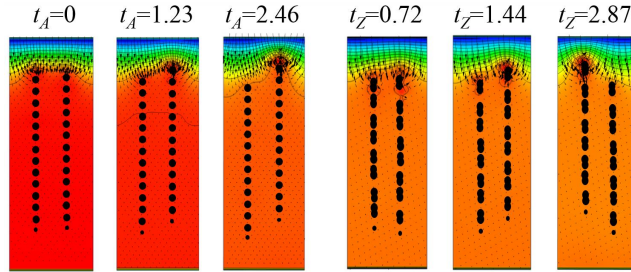


Figure 5: Plots of the average electrostatic potential contour and average electric field vector of bilayer GNRs with the open edge possessing lateral displacement t_X subject to the critical electric field for electron emission. Black dots denote the atomic position.

Table 2: The work function of the bilayer graphene with the closed edges of different curvature radius.

	$X = A$			$X = Z$		
r_X (Å)	1.98	3.17	3.64	2.89	2.93	3.37
Φ (eV)	5.89	4.88	4.79	4.7	4.48	4.75

Since the field emission patterns of the tunneling electrons from the edge of bilayer graphene are associated with the electronic states near the Fermi level, we calculated the local density of state (LDOS) of bilayer graphene with open edges near the Fermi level to simulate the field emission image. The LDOS is calculated by

$$\rho(r) = -\frac{1}{\pi} \text{Im} \sum_{n,k} \int_{E_F - \Delta}^{E_F} dE \frac{|\phi_{n,k}|^2}{E - \epsilon_{n,k} + i\delta}, \quad (2)$$

where Δ is defined as 1 eV and $\phi_{n,k}$ is the valence wave function with the band index n and momentum k . Fig. 7 shows the LDOS of bilayer graphene with various displacement t projected on a plane in a vacuum region. The LDOS of bilayer graphene depends on the edge shape and dislodgment t_X . The emission patterns associated with the upper and lower graphene are observed under the small dislodgment for both armchair and zigzag edges. For the bilayer graphene with the large edge dislodgment, the pattern associated with the protruded edge is dominant. The patterns from the armchair edges show bonding π state natures, while those from the zigzag edges show the dangling bond state and edge state natures.

4.2. Bilayer graphene with closed edges

It has been pointed out that the open edges of multilayered graphene are closed after emitting large current [27]. In this subsection, we investigate how the field emission properties of bilayer graphene depend on the edge closing by calculating the bilayer graphene with closed edge which is simulated by the

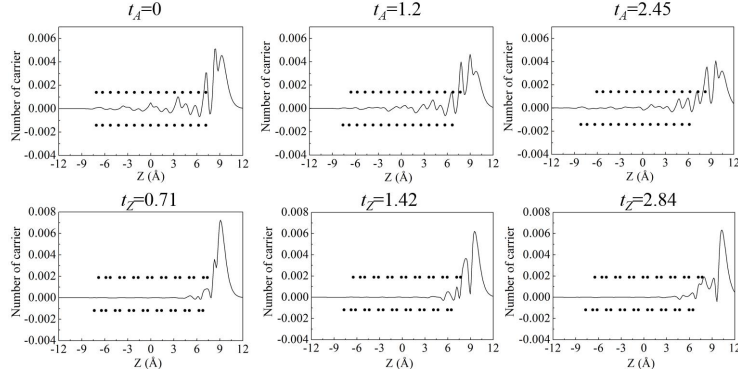


Figure 6: Distribution of accumulated electrons in bilayer GNRs with open edges possessing the lateral displacement t_X under the external electric field corresponding to 0.1 electron doping. Black dots in each panel indicate atomic positions.

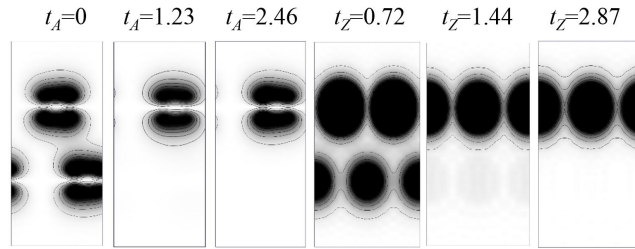


Figure 7: Contour plots of LDOS projected on a plane parallel to the electrode in the vacuum for bilayer GNRs with different t_X under the critical electric field for the electron emission.

folded graphene nanoribbons (Fig. 3). Table 2 summarizes the work functions of bilayer graphene with folded edges whose curvature radius is r_X . Calculated work functions are 5.89, 4.88, and 4.79 eV for the folded armchair edges with the curvature radius of 1.98, 3.17 and 3.64 Å, respectively, and 4.70, 4.48, and 4.75 eV for the folded zigzag edges with the curvature radius of 2.89, 2.93, and 3.37 Å, respectively. We found that the folded armchair edges have larger work function than folded zigzag edges, implying that the folded zigzag edges cause higher field emission current than the folded armchair edges. In addition, we also found that the work functions of the folded edges are smaller than that of the corresponding open edges, except for the case of the folded armchair edge with the curvature radius of 1.98 Å.

Fig. 8 (a) shows the potential barrier for the field emission from the folded graphene edges as a function of the electric field. The potential barrier strongly depends on the electric field intensity and atomic arrangement in the folded moiety, but weakly depends on the curvature of the folded moiety. The potential barrier for all folded edges decreases with increasing the electric field. The folded armchair edges show higher potential barrier than the folded zigzag edges,

180 reflecting their work functions difference. In addition, as the case of the bilayer graphene with the open edge, the potential barrier outside the folded edges are also lower than that outside monolayer graphene.

Fig. 8(b) shows the field emission current from the folded graphene as a function of the electric field, evaluated by Fowler-Nordheim formula shown in the Eq.(1). In accordance with the decrease of the potential barrier with respect to the field, the field emission current increases with increasing the electric field. Emission current from folded edges is larger than that from the open edges of monolayer and bilayer graphene, except the case with a curvature radius of 1.98 Å due to its tightly folded edge. Furthermore, the emission current from the folded edges with zigzag edge is higher than that from the folded edges with armchair edge, irrespective of the curvature of the folded moiety.

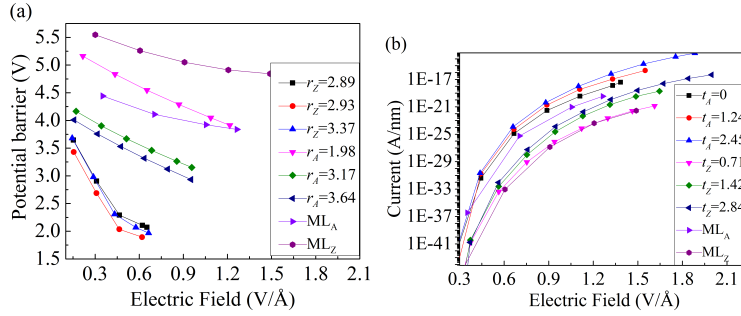


Figure 8: Electric-field dependence of (a) the potential barrier and (b) field emission current for the field emission of folded GNRs and monolayer GNRs with the clean edges.

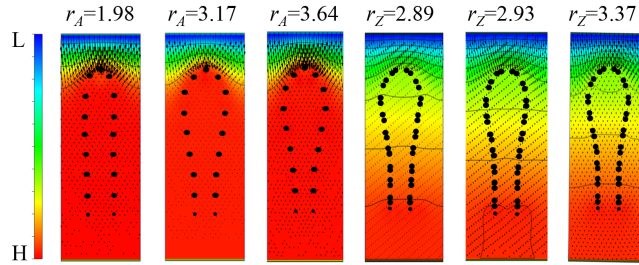


Figure 9: Plots of the average electrostatic potential contour and the average electric field vector of folded GNRs subject to the critical electric field for electron emission. Black dots denote the atomic.

Fig. 9 shows contour plots of electrostatic potential and vector plots of electric field of the folded graphene. For the folded armchair graphene, the electrostatic potential drop occurs between the tip of the folded moiety and the electrode, and the potential monotonically decreases with approaching to the electrode. Accordingly, the electric field mainly concentrates at the tip of the folded region. Note that the field relatively penetrates inside the flat graphitic

region compared with the case of graphene with open edges. The folded moiety of the folded zigzag graphene exhibits unusual feature: the potential gradually decreases between the middle of the graphene ribbon and the folded region, and then it rapidly decreases with approaching the electrode. Therefore, the electric filed highly concentrates around tip of folded region, and simultaneously and substantially penetrates inner region.

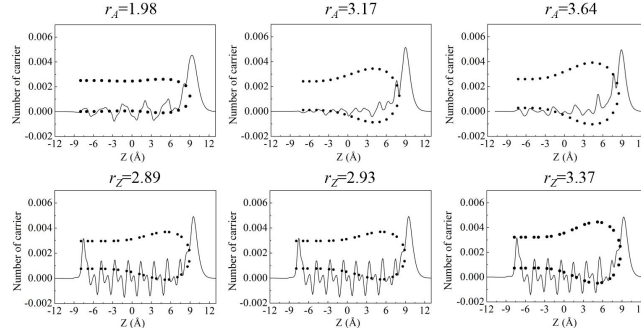


Figure 10: Distribution of accumulated electrons in bilayer GNRs with closed edges under the external electric field corresponding to 0.1 electron doping. Black dots in each panel indicate atomic positions.

To give the physical insight into the unusual potential profile and electric field, we investigate the charge density distribution of accumulated electrons across the folded graphene. Fig. 10 shows the distributions of accumulated electrons in graphene with folded edges under an external electric field, which injects 0.1 electrons to the graphene. We found that the injected carrier primarily accommodated around the folded region, and it has distribution on the flat graphitic region: 75 and 90 % of injected electrons are accommodated around the folded regions of the folded armchair and zigzag graphenes, respectively. The penetrated carriers cause the electric field inner region of graphene. For the case of folded zigzag graphene, the substantial penetration is ascribed to the edge states on the zigzag edge of the graphene opposite to the folded region: the carrier on the atoms at the open edges causes carrier an oscillation in the graphitic region to screen the carrier associated with the edge states.

Finally, we investigate the field emission patterns from the closed edges of bilayer graphene. The pattern is simulated by calculating the LDOS near the Fermi level. Fig. 11 shows the projected images of LDOS for the closed edges of bilayer graphene on a plane in the vacuum region. The field emission pattern of the closed edge of bilayer graphene depends on the atomic arrangements and curvature at the tip of the folded moiety. we found that for each closed edge, the field emission image basically reflects the geometrical structure at the tip of the folded region: H-shaped and hexagonal patterns for closed edges of armchair zigzag graphene, respectively. These characteristic patterns indicate that the field emission of folded graphene is caused by the p_z (or π) electron state of C atoms near the folded moiety.

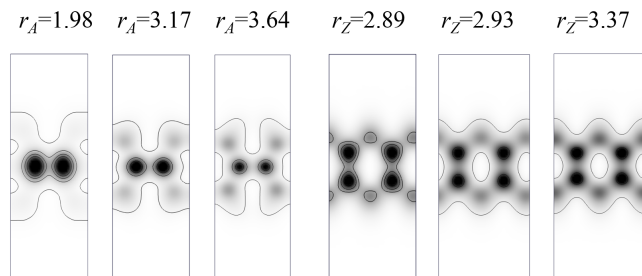


Figure 11: Contour plots of LDOS projected on the plane parallel to the electrode in the vacuum between the folded GNR and electrode for folded GNRs with different curvatures.

5. Conclusion

We studied the electrostatic potential property of bilayer graphene thin films with the open and closed edges under the lateral external electric field based on the DFT combined with ESM method. We found that bilayer graphenes with the open edges have higher field emission current than the corresponding monolayer graphene. Furthermore, the field emission current of bilayer graphene thin films with the open edge can be enhanced by the lateral displacement t_X , irrespective of the edge shape. Besides, the bilayer graphenes with the armchair edges show higher field emission current than those with the zigzag edges due to their lower potential barrier for the field emission caused by their lower work function. For the case with the closed edge, we found that folded edges show higher field emission current compared with the corresponding monolayer graphene and the bilayer graphenes with the open edge. Besides, the folded armchair graphenes have higher potential barrier than the folded zigzag graphene, resulting in their lower field emission current.

Acknowledgments

This work was supported by JST-CREST Grant Numbers JPMJCR1532 and JPMJCR1715 from the Japan Science and Technology Agency, JSPS KAKENHI Grant Numbers JP17H01069, JP16H00898, and JP16H06331 from the Japan Society for the Promotion of Science, and the Joint Research Program on Zero-Emission Energy Research, Institute of Advanced Energy, Kyoto University. Part of the calculations was performed on an NEC SX-Ace at the Cybermedia Center at Osaka University and on an SGI ICE XA/UV at the Institute of Solid State Physics, The University of Tokyo.

References

- [1] V. I. Kleshch, D. A. Bandurin, A. S. Orekhov, S. T. Purcell, A. N. Obraztsov, Edge field emission of large-area single layer graphene, Appl. Surf. Sci. 357 (2015) 1967–1974.

- [2] A. D. Bartolomeo, F. Giubileo, L. Iemmo, F. Romeo, S. Russo, S. Unal, M. Passacantando, V. Grossi, A. M. Cucolo, Leakage and field emission in side-gate graphene field effect transistors, *Appl. Phys. Lett.* 109 (2016) 023510.
- 260 [3] Z. Xiao, J. She, S. Deng, Z. Tang, Z. Li, J. Lu, N. Xu, Field electron emission characteristics and physical mechanism of individual single-layer graphene, *ACS Nano* 4 (2010) 6332–6336.
- [4] J. T. H. Tsai, T. Y. E. Chu, J. Y. Shiu, C. S. Yang, Field emission from an individual freestanding graphene edge, *Small* 8 (2012) 3739–3745.
- 265 [5] C. Wu, F. Li, Y. Zhang, T. Guo, Field emission from vertical graphene sheets formed by screen-printing technique, *Vacuum* 94 (2013) 48–52.
- [6] A. Malesevic¹, R. Kemps, A. Vanhulsel, M. P. C. Chowdhury, V. Alexander, C. V. Haesendonck, Field emission from vertically aligned few-layer graphene, *J. Apply. Phys.* 104 (2008) 084301.
- 270 [7] H. Yamaguchi, K. Murakami, G. Eda, T. Fujita, P. Guan, W. Wang, C. Gong, J. Boisse, S. Miller, M. Acik, K. Cho, Y. J. Chabal, M. Chen, F. Wakaya, M. Takai, M. Chhowalla, Field emission from atomically thin edges of reduced graphene oxide, *ACS Nano* 5 (2011) 4945–4952.
- [8] K. Tada, K. Watanabe, Ab initio study of field emission from graphitic ribbons, *Phys. Rev. Lett.* 88 (2002) 127601.
- 275 [9] M. Araidai, Y. Nakamura, K. Watanabe, Field emission mechanisms of graphitic nanostructures, *Phys. Rev. B* 70 (2004) 245410.
- [10] S. F. Huang, T. C. Leung, B. Li, C. T. Chan, First-principles study of field-emission properties of nanoscale graphite ribbon arrays, *Phys. Rev. B* 72 (2005) 035449.
- 280 [11] Y. Gao, S. Okada, Electrostatic potential barrier for electron emission at graphene edges induced by the nearly free electron states, *Appl. Phys. Express* 10 (2017) 055104.
- [12] Y. Gao, S. Okada, Electrostatic properties of graphene edges for electron emission under an external electric field, *Appl. Phys. Lett.* 112 (2018) 163105.
- 285 [13] Y. Gao, S. Okada, Field emission properties of edge-functionalized graphene, *Carbon* 142 (2019) 190–195.
- [14] Y. Kobayashi, K.-i. Fukui, T. Enoki, K. Kusakabe, Y. Kaburagi, Observation of zigzag and armchair edges of graphite using scanning tunneling microscopy and spectroscopy, *Phys. Rev. B* 71 (2005) 193406.
- 290

- [15] A. C. Ferrari, J. C. Meyer, V. Scardaci, C. Casiraghi, M. Lazzeri, F. Mauri, S. Piscanec, D. Jiang, K. S. Novoselov, S. Roth, A. K. Geim, Raman spectrum of graphene and graphene layers, *Phys. Rev. Lett.* **97** (2006) 187401.
- 295 [16] Y. Kobayashi, K.-i. Fukui, T. Enoki, Edge state on hydrogen-terminated graphite edges investigated by scanning tunneling microscopy, *Phys. Rev. B* **73** (2006) 125415.
- [17] J. C. Meyer, A. K. Geim, M. I. Katsnelson, K. S. Novoselov, D. Obergfell, S. Roth, C. Girit, A. Zettl, On the roughness of single- and bi-layer
300 graphene membranes, *Solid State Commun.* **143** (2007) 101–109.
- [18] Z. Liu, K. Suenaga, P. J. F. Harris, S. Iijima, Open and closed edges of graphene layers, *Phys. Rev. Lett.* **102** (2009) 015501.
- [19] H.-V. Roy, C. Kallinger, K. Sattler, Study of single and multiple foldings of graphitic sheets, *Surface Science* **407** (1998) 1–6.
- 305 [20] K. Kim, Z. Lee, B. D. Malone, K. T. Chan, B. Aleman, W. Regan, W. Gannett, M. F. Crommie, M. L. Cohen, Z. A., Multiply folded graphene, *Phys. Rev. B* **83** (2011) 245433.
- [21] P. Hohenberg, W. Kohn, Inhomogeneous electron gas, *Phys. Rev. B* **136** (3B) (1964) B864.
- 310 [22] W. Kohn, L. J. Sham, Self-consistent equations including exchange and correlation effects, *Phys. Rev.* **140** (4A) (1965) 1133–1138.
- [23] Y. Morikawa, K. Iwata, K. Terakura, Theoretical study of hydrogenation process of formate on clean and Zn deposited Cu (111) surfaces, *Appl. Surf. Sci.* **169–170** (2001) 11–15.
- 315 [24] J. P. Perdew, K. Burke, M. Ernzerhof, Generalized gradient approximation made simple [*Phys. Rev. Lett.* **77**, 3865 (1996)], *Phys. Rev. Lett.* **78** (7) (1997) 1396.
- [25] D. Vanderbilt, Soft self-consistent pseudopotentials in a generalized eigenvalue formalism, *Phys. Rev. B* **41** (11) (1990) 7892–7895.
- 320 [26] A. Yamanaka, S. Okada, Energetics and electronic structure of graphene nanoribbons under a lateral electric field, *Carbon* **96** (2016) 351–361.
- [27] K. Nakakubo, K. Asaka, H. Nakahara, Y. Saito, Field emission from vertically aligned few-layer graphene, *Appl. Phys. Express* **5** (2012) 055101.